Desalination and Water Treatment
www.deswater.com
doi: 10.1080/19443994.2013.803265

52 (2014) 4508–4519
June

Taylor & Francis
Taylor & Francis Group

Utilization of bottom ash as a low-cost sorbent for the removal and recovery of a toxic halogen containing dye eosin yellow

Jyoti Mittal[a,*], Damodar Jhare[a], Harsh Vardhan[b], Alok Mittal[a]

[a]*Department of Chemistry, Maulana Azad National Institute of Technology, Bhopal 462 051, India*
Tel. +91 9893251369; Fax: +91 755 2670562; email: jyalmittal@yahoo.co.in
[b]*Department of Chemistry, Mihir Bhoj (PG) College, GB Nagar, Dadri, UP, India*

Received 20 April 2013; Accepted 26 April 2013

ABSTRACT

Removal and recovery of a hazardous halogen-containing dye Eosin Yellow were investigated using Bottom Ash as adsorbent. During the studies various essential factors influencing the adsorption, like sieve size of adsorbent, adsorbate concentration, amount of adsorbent, pH of the solution, contact time, and temperature have been monitored. Attempts have also been made to verify Langmuir, Freundlich, Tempkin, and D-R adsorption isotherm models. The feasibility of the ongoing adsorption has been ascertained on the basis of Langmuir adsorption isotherm. The free energy, entropy, and enthalpy of the ongoing adsorption process have been evaluated as about 26 kJ mol^{-1}, 22 kJ mol^{-1}, and 20 kJ mol^{-1}, respectively. Contact time studies reveal that the ongoing adsorption equilibrate within 3 h of contact. It is found that the adsorption of Eosin Yellow over Bottom Ash follows a pseudo-second-order kinetics. At all the temperatures rate constant of the process was calculated around 5×10^{-8} sec g mol^{-1}. During bulk removal through column operation about 97% percentage saturation of the dye is obtained. Desorption studies exhibit that the percentage recovery of Eosin Yellow dye on eluenting NaOH solution through exhausted column is about 90%.

Keywords: Eosin Yellow; Bottom Ash; Adsorption; Isotherms; Kinetics; Column Studies

1. Introduction

A safe, healthy, and disease free drinking water is an essential prerequisite for the existence of humanity but unfortunately with the rapid increase in population and industrialization the water quality is diminishing day by day. Effluents emerging out from various industries contain large number of toxic substances like acids, alkalis, metal ions, dyes, pigments, etc. Out of all these contaminants, dyes are present in larger proportion and considered as most dangerous for humans, animals, and aquatic creatures [1].

The presence of dye molecules in water is mainly due to discharge of textile, paper, rubber, plastics, cosmetics, printing, etc. industries and it guesstimated that every year more than 150 thousand tons of different types of dyes are released by these industries into water [2]. The dye molecules are not only visible by naked eyes but also highly stable to light and heat [3], which makes their removal difficult by any ordinary chemical or physical method and, therefore, utmost care is needed to select a suitable method during

*Corresponding author.

wastewater treatment process [4]. In recent years processes, such as electrochemical [5], membrane filtration, biosorption [6,7] ion-exchange [8], photocatalytic degradation [9], coagulation/flocculation [10], electrocoagulation [11], ozonation [12], etc. have been applied. But it is found that either the method is expensive or do not eradicate the dye completely. The treatment by electrochemical or photochemical methods also pose problems of generation of some toxic by-products or intermediates. The hunt of a safe, economic, fast, and most suitable water treatment process finally concluded at adsorption technique and for the last two decades this technique has established as the most powerful tool in the water treatment technology [13–21]. The economics and versatility of adsorption process are largely dependent upon the adsorbent material and various low-cost adsorbents, such as pith, chitin, chitoson, sunflower stalk, rice husk, aloe barbadensis, coconut shell, tea leaves, and sugar cane bagasse [22–26], etc. have been used by researchers for the removal of dyes from wastewater. Present paper is yet another attempt to formulate a process to remove a hazardous highly water-soluble halogen-containing fluorescein dye, Eosin Yellow using waste material Bottom Ash as a suitable adsorbent.

The dye Eosin Yellow exists in the red crystalline form and with solubility of 400 g/L in water, it poses excellent stability in air. It is used to color variety of materials, such as textile materials, ink, gasoline, drugs and pharmaceutics, cosmetics, etc. [27]. Despite its usefulness in these industries, the dye is highly toxic and can even carcinogenic to humans [28]. It can cause skin and eye irritations and can inhibit growth of corneal epithelial cells of eyes [29]. This dye is also found to inhibit the binding efficiency of protein in liver and can create geno-toxicity in human organs [30,31]. Thus, the thoughtful attempt to develop a process for its removal from water is useful and necessary for the mankind.

The adsorbent Bottom Ash is a waste material, which has been efficiently used for the removal of various types of inorganic and organic pollutants from wastewater by this laboratory as well as by several other workers [32]. It is the unburned waste material of the thermal coal power generation plant that remains in the bottom of the incinerator furnace. Though it is neither hazardous nor toxic to the humans, insects, and animals but its continuous generation requires a regular disposal, which is a matter of great concern to the plant authorities as it makes the agriculture land barren, infertile, and unproductive [33]. This research article presents the attempt made in our laboratory to utilize Bottom Ash as a potential adsorbent for the removal and recovery of toxic Eosin Yellow dye.

2. Experimental

2.1. Material and methods

Eosin Yellow (Fig. 1) having IUPAC name, 2-(2,4,5,7-tetrabromo-6-oxido-3-oxido-3H xanthenes-9-yl) benzoate disodium salt and molecular formula $C_{20}H_6Br_4Na_2O_5$ (molecular weight 691.88), was obtained from M/s Merck. Its 0.01 M stock solution was prepared in double distilled water. All other reagents used were of analytical reagent grade.

The dark gray colored granules of adsorbent material Bottom Ash were obtained from thermal power station of M/s bharat heavy electrical limited, Bhopal (India). A microprocessor based pH meter model HI 8424 (M/s Henna Instruments, Italy) was used for pH measurements and all adsorption studies were monitored by using UV/Visible spectrophotometer model 117 (Systronics, Ahmedabad, India).

Different instruments were used for characterizing physical and chemical property of Bottom ash. Scanning Electron Microscopy was performed on Philips SEM 501 electron microscope, while X-ray measurements were carried out on Philips X-ray diffractophotometer employing Nickel filtered Cu-α-radiations. Quantasorb model QS-7 surface analyzer was used to calculate the surface of the adsorbent particles. The pore properties and specific gravity of the adsorbent was determined by employing a mercury porosimeter and specific gravity bottles, respectively.

2.2. Material development

The Adsorbent material Bottom Ash was first ground into fine particles and washed with double distilled water several times and then dried. The dry material is then treated with hydrogen peroxide solution (30% w/v) at room temperature for 24 h to oxidize the adhering organic impurities and then washed with double distilled water. To remove the moisture, resulting material was dried in an oven at 100°C for about 1 h. The dried material was then kept in muffle furnace at 500°C for 15 min. The activated Bottom Ash thus obtained was then sieved to desired particle size,

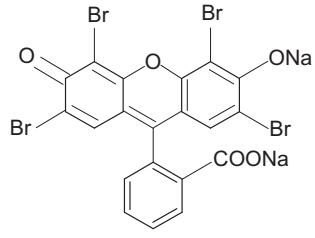

Fig. 1. Structure of eosin yellow.

such as 0.425–0.150 mm (36 BSS Mesh), 0.150–0.088 mm (100 BSS Mesh), and ⩽0.088 mm (170 BSS Mesh) and stored in separate vacuum desiccators.

2.3. Adsorption studies

During batch studies, 25 mL of dye solution of known concentration was taken in a 100 mL of volumetric flask and fixed amount of Bottom Ash of a particular mesh size was added into it at a fixed temperature (30, 40, and 50°C) and pH. The solution is now agitated by a mechanical shaker for a predetermined time to attain the equilibrium. When the equilibrium was thought to be established, the solution was filtered through Whattman filter paper (no. 41) and the amount of the dye uptake was analyzed spectrophotometrically at $\lambda_{max} = 516$ nm.

2.4. Kinetic studies

Kinetic studies were also carried out by batch technique. During kinetic study, in a series of airtight 100 mL volumetric flasks 25 mL dye solution of desired concentration and pH was taken in each and known amount of the adsorbent of a fixed sieve size was added into these. Each flask was agitated on mechanical shaker for a fixed time interval and removed one by one to analyze the filtrate spectrophotometrically to determine the dye uptake.

2.5. Column studies

Column studies were carried out in a glass column of 30 cm length and 1 cm internal diameter. In order to prepare bed of the adsorbent, slurry of 1 g Bottom Ash of 100 BSS Mesh size was prepared in double distilled water and kept overnight untouched. By keeping the outlet of the glass column open, the slurry was slowly fed into it on a glass wool support. This created a homogeneous bed of the adsorbent Bottom Ash at the bottom of glass column, on the glass wool support. To avoid any air entrapment in the column the water of the slurry was continuously percolate through the column outlet. The column thus prepared was then loaded with dye solution of 10×10^{-5} M concentration of Eosin Yellow and percolated at a constant flow rate of 0.5 mL/min. In various test tubes collection of 10 mL quantity of effluent was made and dye concentration in each test tube was analyzed by UV/Visible spectrophotometer. When the concentration of the dye solution fed into the column and collected as effluent was found equal, the adsorbent bed was considered completely exhausted and column operation was shut down.

2.6. Desorption and column regeneration

In order to recover the dye material from the exhausted bed of the adsorbent, desorption operation was carried out in the same column and aliquots of dilute NaOH solution were eluted through the column at a constant flow rate of 0.5 mL/min. Effluent containing dye along with NaOH was collected in a flask at the outlet of the column. When completed dye was drained out, the adsorbent bed of the column was properly washed with hot water and the column was now ready for the next cycle of operation.

3. Result and discussion

3.1. Characterization of adsorbent

The chemical characteristics of the activated Bottom Ash were determined by using standard analytical procedures [34]. The details of the constituents of the adsorbent materials as per standard physical parameters, like surface area, porosity, density, and loss of ignition of the activated Bottom Ash were obtained as 870.5 $cm^2 g^{-1}$, 46%, 0.6301 $g ml^{-1}$, and 1.14%, respectively. It was found that in the analyzed Bottom Ash sample SiO_2, CaO, Al_2O_3, Fe_2O_3, MgO, Na_2O, and moisture were present 45.4, 15.3, 10.3, 9.7, 3.1, 1.0, and 15% by weight, respectively.

To evaluate the nature of Bottom Ash, its weighted amount was added into 25 mL of distilled water, at pH 7.0 and stirred thoroughly. The solution was kept undisturbed for 24 h in the 100 mL airtight conical flask and then filtered to measure the pH. The pH value was found to decrease which confirmed the acidic nature of the Bottom Ash.

SEM photographs ascertained that the particulates of Bottom Ash are almost spherical and porous in nature. DTA curves of Bottom Ash were found thermally stable and negligible weight loss even at high temperatures. The X-ray diffraction spectra indicates the presence of Alumina (Al_2O_3), Gypsum ($CaSO_4.2H_2O$), Beaverite [$Pb(Cu,Fe,Al)_3(SO_4)_2(OH)_6$], Borax ($Na_2B_4O_7.10H_2O$), and Kaolinite [$2\{Al_2Si_2O_5(OH)_4\}$] in the activated Bottom Ash. Infrared Spectroscopy helped in determination of the adsorptive nature of the adsorbent. Bottom Ash gave a sharp adsorption band in 790 cm^{-1} region, corresponding to Kaolinite [$2\{Al_2Si_2O_5(OH)_4\}$]. The bands at 3,467, 2,930, 2,676, 1,502, 1,097, 470.2, and 790 cm^{-1} confirmed the presence of Laumonite [$4CaAl_{42}Si_4O_{12}.4H_2O$], Amber, Mulite [$3Al_2O_3.2SiO_2$], Azurite [$Cu_3(CO_3)_2(OH)_2$], Bavenite [$4Ca_4(BeAl)_4Si_9(O.OH)_{29}(OH)_2$], Gypsum [$3(CaSO_4.2H_2O)$], and Corundum [$2(\alpha\text{-}Al_2O_3)$] respectively. Similar results were found in earlier study also [35–37].

3.2. Adsorption studies

3.2.1. Effect of pH of solution

The effect of pH on the adsorption of Eosin Yellow dye was monitored in the pH range 3–12, at initial dye concentration of 1×10^{-4} M and 100 BSS Mesh size of adsorbent at temperature 30, 40, and 50°C. The pH of the test solutions were adjusted by adding dilute hydrochloric acid and dilute sodium hydroxide. It was found that in each case with the decrease in the pH of the dye solution the dye uptake decreased almost linearly. Fig. 2 depicts the effect of pH on the removal of Eosin Yellow by Bottom Ash at 30°C.

3.2.2. Effect of adsorbate concentration and temperature

The adsorption experiments were carried out in the concentration range of the dye ranging from 1×10^{-5} to 10×10^{-5} M, at pH 7.0 and temperatures 30, 40, and 50°C. Fig. 3 clearly depicts that the amount of the dye adsorbed increases with the increase in dye concentration. It was also found that the rate of removal of the Eosine Yellow is faster at high concentration and increases with concentration and temperature. An increase in adsorption of the dye with rising temperature reveals the endothermic nature of the ongoing adsorption process.

3.2.3. Effect of amount and sieve size of adsorbent

To study the effect of amount of adsorbent on the removal of Eosin Yellow the amount of grinded Bottom ash of a particular sieve size was varied from 0.05 to 0.50 g at fixed pH, concentration and temperatures 30, 40, and 50°C. Table 1 exhibits that the adsorption of the dye increases by increasing the amount of adsorbent. It was also found that when the amount of adsorbent increased from 0.10 to 0.25 g, the adsorption capacity increased to almost double.

The batch adsorption experiments were also carried out to investigate the effect of mess size. During the study, three different particles size viz. 36, 100, and 170 BSS Mesh were taken at a fixed pH, initial concentration of the dye, amount of adsorbent, and different temperature. It was observed that the uptake of the dye increased with decreasing particle size and amount of adsorption achieved for 36, 100, and 170 BSS Mesh sizes were 0.343×10^{-5}, 0.531×10^{-5}, and 0.595×10^{-5} Mol/g.

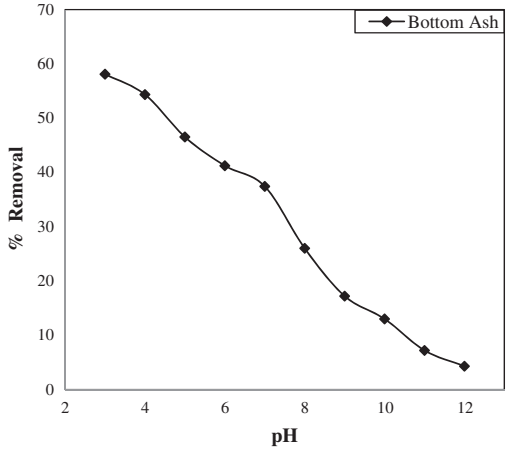

Fig. 2. Effect of pH on the eosin yellow (Concentration = 1×10^{-4} M) - bottom ash (amount = 0.25 g & mesh size = 100 BSS) system at 30°C.

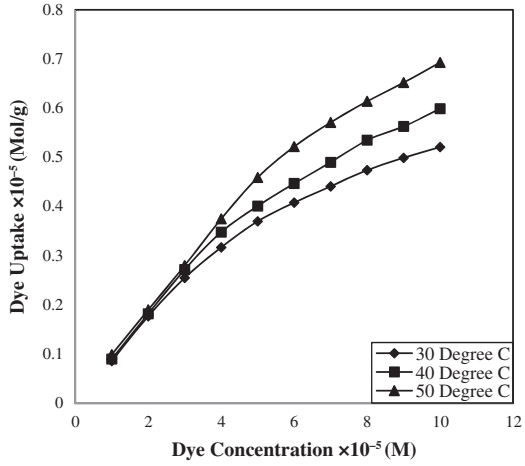

Fig. 3. Effect of concentration of eosin yellow (pH = 7.0) on the adsorption over bottom ash (amount = 0.25 g & mesh size = 100 BSS) at different temperatures.

Table 1
Effect of amount of Bottom Ash (100 BSS mesh) on the adsorption of Eosin Yellow (concentration 1×10^{-4} & pH = 7.0) at different temperatures

Amount of bottom ash (g)	Amount of eosin yellow adsorbed $\times 10^{-6}$ (g)		
	30°C	40°C	50°C
0.05	0.124	0.154	0.224
0.10	0.170	0.241	0.358
0.15	0.407	0.712	0.946
0.20	0.775	1.155	1.579
0.25	1.170	1.475	1.913
0.30	1.361	1.974	2.200
0.35	1.590	2.048	2.358
0.40	1.816	2.137	2.429
0.45	2.004	2.299	2.475
0.50	2.167	2.325	2.493

3.2.4. Effect of contact time

Contact time studies are helpful in understanding the amount of dye adsorbed at various time intervals. Contact time studies were performed at the dye concentration 7×10^{-5} M at fixed pH, amount of adsorbent, BSS Mesh size, and temperatures. Fig. 4 shows that in the present case equilibrium was achieved in almost 90 min of contact time and about 10.32, 11.95, and 12.39 mg per gram of dye was adsorbed at 30, 40, and 50°C temperatures, respectively. It was also found that the adsorption capacity increased with increase in the temperature, which once again confirmed the endothermic nature of adsorption process.

3.3. Kinetic studies

3.3.1. Adsorption rate constant study

The kinetic study of the dye Eosin Yellow – Bottom Ash adsorption was monitored through various kinetic models and it was established that the ongoing adsorption follows a pseudo-second-order process. Following Ho-Mckay [38] pseudo-second-order rate expression was applied to calculate the specific rate constant of the ongoing adsorption:

$$\frac{t}{q_t} = \frac{1}{k_2 q_e^2} + \frac{t}{q_e} \tag{1}$$

where q_e and q_t are the adsorption capacities (Mol/g) at equilibrium and time t (Sec), respectively, and k_2 is the rate constant of the pseudo-second order-rate expression (sec g Mol^{-1}).

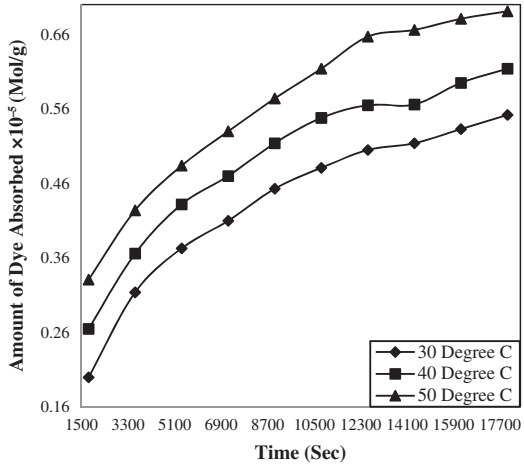

Fig. 4. Effect of contact time on the eosin yellow (pH = 7.0, concentration = 7×10^{-5} M) Adsorption over bottom ash (Amount = 0.25 g & mesh size = 100 BSS) at different temperatures.

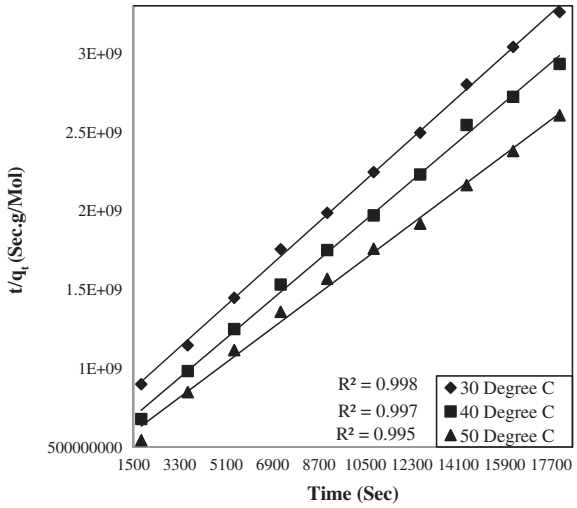

Fig. 5. Time vs. t/q_t plot for Eosin Yellow (pH = 7.0, concentration = 7×10^{-5} M)—Bottom Ash (amount = 0.25 g & mesh size = 100 BSS) system at different temperatures.

The kinetic measurements were carried out in 7×10^{-5} M concentration of the dye using 0.25 g of Bottom Ash in the solution. The plot of t/q_t against time (Fig. 5) gives straight lines with regression coefficient values equivalent to almost unity, confirming thereby the pseudo-second-order kinetics of the ongoing process at all the temperatures. The rate constant for the process was found almost 5×10^{-8} sec g Mol^{-1} at all the temperatures.

3.3.2. Rate expression and treatment of data

The interpretation of the experimental data monitoring the overall rate of adsorption of Eosin Yellow over Bottom ash was carried out using the mathematical treatment recommended by Boyd [39] and Reichenberg [40]. These mathematical treatments were employed to distinguish particle diffusion with film diffusion process involved in the ongoing adsorption. The theoretic aspects of these models have already been presented elsewhere [36,37], while the quantitative treatment of the adsorption can be monitored through the following expressions:

$$F = 1 - \frac{6}{\pi^2} \sum_{1}^{\infty} (1/n^2) \exp(-n^2 B_t) \tag{2}$$

where "n" is Freundlich constant and "F" is the fractional attainment of equilibrium at time"t" and is obtained by using following equation:

$$F = \frac{Q_t}{Q_\infty} \tag{3}$$

where Q_t and Q_∞ are amounts adsorbed after time t and after infinite time, respectively. The other parameter "B_t" is known as time constant and obtained by following expression:

$$B_t = \frac{\pi^2 D_i}{(r_o^2)} \tag{4}$$

where B_t is the time constant, D_i is the effective diffusion coefficient of adsorbate in the adsorbent phase and r_o is the radius of adsorbent particles assumed to be spherical.

For every observed value of F, corresponding values of B_t were derived from Reichenberg's table. Graph B_t vs. time plotted for 7×10^{-5} M dye solution was found to be non linear and do not pass through the origin, which reveals that the rate determining process is governed through film diffusion and maximum adsorption is taking place over the external surface of adsorbent.

For the ongoing adsorption, the values of effective diffusion coefficient D_i were also calculated at 30, 40, and 50 °C with the help of slopes of time vs. B_t graphs. The energy of activation (E_a), entropy ($\Delta S^{\#}$) and pre-exponential constant (D_o), values were calculated using the following equations:

$$D_i = D_o \exp\left(-\frac{E_a}{RT}\right) \tag{5}$$

$$D_o = (2.72 d^2 KT/h) \exp\left(-\frac{\Delta S^{\#}}{R}\right) \tag{6}$$

In the equations given above D_o is the pre–exponential constant, $\Delta S^{\#}$ is the entropy, d gives the average distance between the two successive sites of the adsorbent, h is the Planks constant; k, Boltzmann constant; E_a, the energy of activation; T is the temperature and R is the universal gas constant. The values of these parameters obtained in the present case are presented in Table 2. The decreasing values of effective diffusion coefficient (D_i) with respect to increase in the temperature (Fig. 6) clearly establishes that the mobility of the ions decreases due to increased retarding force acting on diffusing particles of the dye. The negative values of $\Delta S^{\#}$ obtained from the systems reveal that the internal structure of the Bottom Ash do not go through any significant change during adsorption of the dye.

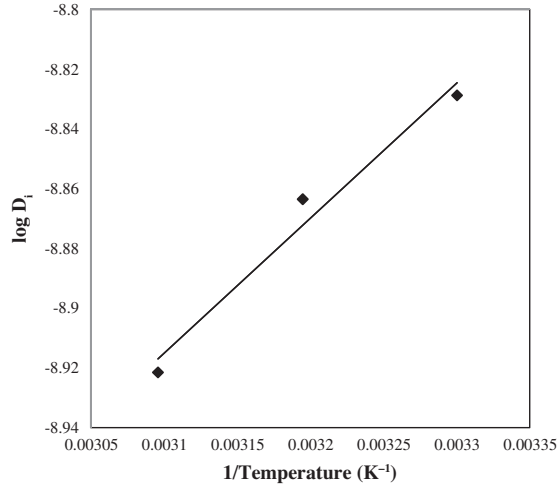

Fig. 6. $1/T$ vs. log D_i plot for the Eosin Yellow (pH = 7.0, concentration = 7×10^{-5} M)—Bottom Ash (0.25 g & mesh size = 100 BSS) system at different temperatures.

3.4. Adsorption isotherms models

Relation between the amount of dye adsorbed by a unit weight of adsorbent and remaining concentration of the dye in the solution is described by various forms of adsorption isotherms [41]. In the present work, well-known Freundlich, Langmuir, Tempkin, and D–R isothermal models have been applied to draw various parameters related to the ongoing adsorption.

3.4.1. The Langmuir adsorption isotherm model

Following linear equation of Langmuir adsorption isotherm is used to ascertain uniform monolayer development on the surface of Bottom Ash:

$$\frac{1}{q_e} = \frac{1}{Q_o} + \frac{1}{bQ_oC_e} \tag{7}$$

Table 2
Values of effective diffusion coefficient (D_i), pre exponential constant (D_o), activation energy (E_a) and entropy of activation ($\Delta S^{\#}$) for the diffusion of eosin yellow adsorption over bottom ash

$D_i \times 10^{-9}$			D_o	E_a	$-\Delta S^{\#}$
30 °C	40 °C	50 °C		(kJ mol^{-1})	(J K^{-1} mol^{-1})
1.4833	1.3692	1.1980	4.90×10^{-11}	3.748	477.764

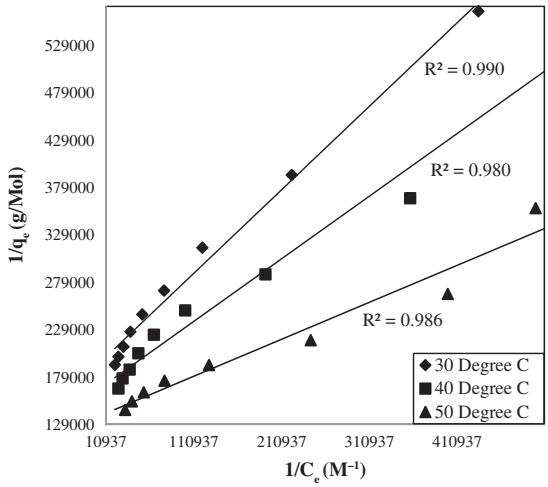

Fig. 7. Langmuir isotherms for the Eosin Yellow (pH = 7.0) adsorption over Bottom Ash (amount = 0.25 g & mesh size = 100 BSS).

where q_e is the amount of dye adsorbed (mol/g), C_e is the equilibrium molar concentration of the dye (mol/ L), Q_o is the maximum adsorption capacity (mol/g), and b is the energy of adsorption (L/mol).

To verify Langmuir isotherm model, the $1/C_e$ vs. $1/q_e$ were plotted at temperatures 30, 40, and 50°C and straight lines with appreciable R^2 values were obtained at all the temperatures (Fig. 7). This behavior verifies the Langmuir adsorption model and involvement of monolayer adsorption on each temperature. The straight lines obtained are also helpful in calculating the Langmuir constant "*b*" and number of moles of the dye adsorbed per unit weight of the adsorbent (Q_o) through their slopes and intercepts, respectively (Table 3).

3.4.2. Thermodynamic parameters and feasibility of the process

With the help of Langmuir constant "*b*" various thermodynamic parameters, such as change in standard free energy (ΔG°), change in enthalpy (ΔH°), and change in entropy (ΔS°) were calculated by using following relations:

$$\Delta G^o = -RT \ln b \tag{8}$$

$$\Delta H^o = -R \frac{T_2 T_1}{T_2 - T_1} \times \ln \frac{b_2}{b_1} \tag{9}$$

$$\Delta S^o = \frac{\Delta H^o - \Delta G^o}{T} \tag{10}$$

The values of these thermodynamic parameters are presented in Table 4. The negative values of ΔG° indicate spontaneous nature of the adsorption process at all the temperature, while positive value of ΔH° further confirms endothermic nature of ongoing process. Increase in the degree of randomness over the surface of adsorbent Bottom Ash during adsorption process was ascertained by increase in the value of ΔS°.

Table 3
Values of different adsorption isotherm constants for eosin yellow (pH = 7.0)—bottom ash (amount = 0.25 g & mesh size = 100 BSS) system at different temperatures

Langmuir constants					
$Q_o \times 10^{-5}$ (mol/g)			$b \times 10^{-3}$ (L/mol)		
30°C	40°C	50°C	30°C	40°C	50°C
5.23	6.07	7.32	21.66	24.92	35.01
Freundlich constants					
n			$K_F \times 10^{-4}$		
30 °C	40°C	30°C	40°C	30°C	40°C
2.949	2.941	2.949	2.941	2.949	2.941
Tempkin constants					
$k_1 \times 10^{-6}$ (L/mol)			$k_2 \times 10^{8}$		
30°C	40°C	30°C	40°C	30°C	40°C
1.0	1.0	1.0	1.0	1.0	1.0
D-R constants					
$-\beta$ (mol^2 J^{-2}) $\times 10^{-9}$			X_m (mol/g) $\times 10^{-5}$		
30°C	40°C	30°C	40°C	30°C	40°C
2.0	2.0	2.0	2.0	2.0	2.0

Table 4
Values of thermodynamic parameters for Eosin Yellow (pH 7.0)—Bottom Ash (amount = 0.25 g and mesh size = 100 BSS) system at different temperatures

$-\Delta G^o$ (kJ mol^{-1})			ΔH^o (kJ mol^{-1})	ΔS^o (J K^{-1} mol^{-1})
30℃	40℃	50℃	19.727	21.756
25.149	26.344	28.099		

A dimensionless separation factor "*r*" [42] was also calculated to measure the feasibility and favorability of the ongoing adsorption process, by using following expression:

$$r = \frac{1}{1 + bC_o} \tag{11}$$

where b is the Langmuir constant and C_o is the initial concentration. The values of "*r*" were found as 0.31, 0.28, and 0.22 at 30, 40, and 50℃, respectively. Less than 1 values of 'r' at all the temperatures suggest highly favorable adsorption during the ongoing process.

3.4.3. The Freundlich adsorption isotherm model

The validity of the Freundlich isotherm model was proved by using following relation:

$$\log q_e = \log K_F + (1/n) \log C_e \tag{12}$$

where q_e is the amount adsorbed (mol/g), C_e is the equilibrium concentration of the adsorbate (mol/L). K_F and n the Freundlich constants, are related to adsorption capacity and adsorption intensity, respectively. The graph plotted log C_e vs. log q_e, gave straight lines with regression coefficients close to unity (Fig. 8) thereby verifying the Freundlich adsorption model. Values of K_F and n were derived from the intercepts and slope of these straight lines, respectively and presented in Table 3.

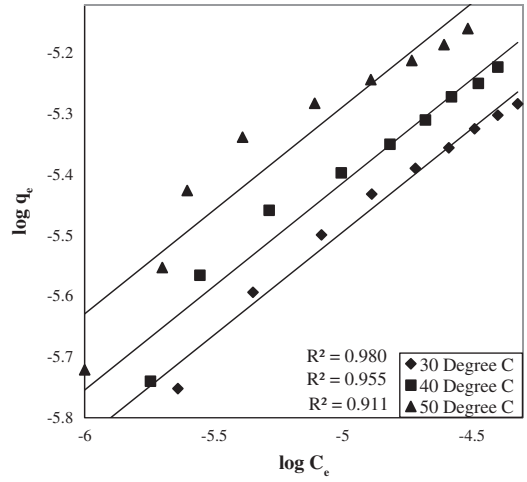

Fig. 8. Freundlich isotherms for the Eosin Yellow (pH = 7.0) adsorption over Bottom Ash (amount = 0.25 g & mesh size = 100 BSS).

3.4.4. The Tempkin adsorption isotherm model

The evaluation of heat of adsorption of all the molecules increases linearly with the coverage of the adsorbate particles over adsorbent and such a phenomenon is studied by Tempkin adsorption isotherm model. The linear form of the model is expressed as:

$$q_e = k_1 \ln k_2 + k_1 \ln C_e \tag{13}$$

where q_e is the amount adsorbed at equilibrium in (mol/g), C_e is the equilibrium concentration of the adsorbate (mol/L), k_1 is the Tempkin isotherm energy constant (L/mol) related to the heat of adsorption, and k_2 is the Tempkin's isotherm constant. Thus, ln C_e vs. q_e graphs were drawn at all the temperatures which gave straight lines (Fig. 9) indicating thereby

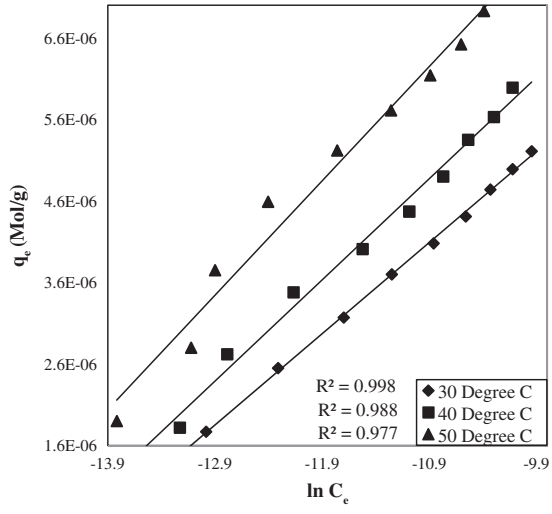

Fig. 9. Tempkin Isotherms for the Eosin Yellow (pH = 7.0) adsorption over Bottom Ash (amount = 0.25 g & mesh size = 100 BSS).

uniform distribution of binding energy. These straight lines were also helpful in determining the Tempkin isotherm constants—k_1 and k_2 and value of these constants are presented in Table 3.

3.4.5. D–R adsorption isotherm model

To diagnose whether the ongoing adsorption is through physical interaction (physisorption) or chemical bonding (chemisorption), following linear form of D–R adsorption isotherm model was applied:

$$\ln C_{ads} = \ln X_m - \beta\varepsilon^2 \tag{14}$$

where C_{ads} is the amount of the dye adsorbed per unit weight of the adsorbent in (mg/g), X_m is the maximum sorption capacity provided by the intercept in (μmol/g), β is the activity coefficient related to mean sorption energy (mol^2/J^{-2}), and ε is the Polanyi potential, which is equal to:

$$\varepsilon = RT\ln\left(1+\frac{1}{C_e}\right) \tag{15}$$

where R is the gas constant and T is temperature in Kelvin. The activity coefficient (β) and the adsorption capacities (ln X_m) were evaluated from the slopes and intercepts of the ln C_{ads} vs. ε^2 graph (Fig. 10) at 30, 40, and 50°C, respectively and results are depicted in Table 3. The mean sorption energy was evaluated by following expression:

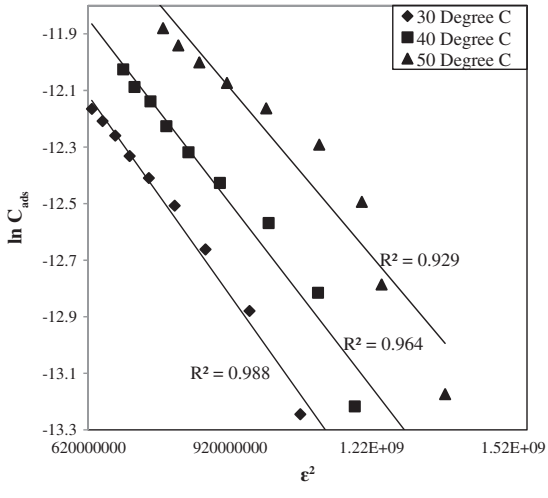

Fig. 10. D-R isotherms for the Eosin Yellow (pH = 7.0) adsorption over Bottom Ash (amount = 0.25 g & mesh size = 100 BSS).

$$E = \frac{1}{\sqrt{-2\beta}} \tag{16}$$

At all the temperatures the values of E were found 15.8 kJ, indicating thereby involvement of "Chemisorption" in the present adsorption process [43].

3.5. Column studies

In order to develop an industrial friendly method the bulk removal of the dye was carried out by using a continuous flow technique involving fixed–bed column operation [44,45]. This method is quite easy to operate and provides many useful parameters related to dye removal [45].

In the present studies, parameters like length of primary adsorption zone (δ), time involved in establishing the primary adsorption zone (t_x), time required by primary adsorption zone to move down its length (t_δ), time of initial formation of primary adsorption zone (t_f), fractional capacity of the prepared column (f), mass rate of flow to the adsorbent (F_m), and percent saturation of column at break point were calculated by using following expressions:

$$t_x = \frac{V_x}{F_m} \tag{17}$$

$$t_\delta = \frac{V_x - V_b}{F_m} \tag{18}$$

$$\frac{\delta}{D} = \frac{t_\delta}{t_x - t_f} = \frac{t_\delta}{t_x + t_\delta(f-1)} = \frac{V_x - V_b}{V_b + f(V_x - V_b)} \tag{19}$$

$$f = 1 - \frac{t_f}{t_\delta} = \frac{Ms}{(V_x - V_b)C_o} \tag{20}$$

$$\text{Percentage saturation} = \frac{D + \delta(f-1)}{D} \tag{21}$$

where Ms. is the amount of adsorbate adsorbed in the primary adsorption zone from break point to exhaustion, C_o is initial concentration of adsorbate, and D is the length of column.

3.5.1. Column adsorption

In the present study the column operation were operated at 10×10^{-5} M dye concentration and the solution was pass through the column at a flow rate of 0.5 mL/min and breakthrough curve was drawn by collecting 130 mL drained out solution of Eosin Yellow

Table 5
Values of fixed bed adsorber parameters for the adsorption of Eosin Yellow over Bottom Ash in a glass column

C_o (M)	C_x (M)	C_b (M)	V_x (mL)	V_b (mL)	$(V_x - V_b)$ (mL)	F_m (mg/cm^2/min)	D
10×10^{-5}	0.67×10^{-5}	9.48×10^{-5}	100	30	70	0.0440	1.0

Table 6
Values of fixed bed adsorber parameters for the adsorption of Eosin Yellow over Bottom Ash in a glass column

t_x (min)	t_δ (min)	t_f (min)	f	δ (cm)	Percentage saturation
2269.18	1588.42	60	0.962	0.7161	97.29

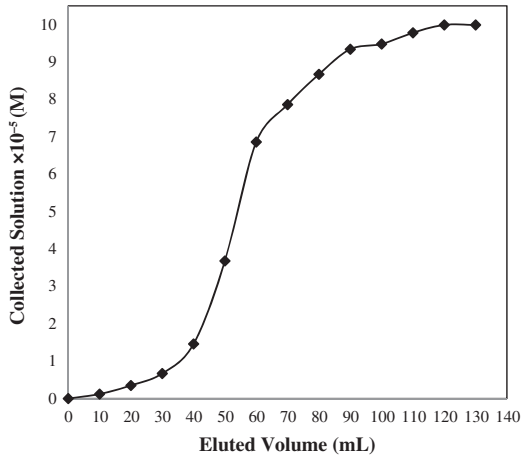

Fig. 11. Breakthrough curve for the column operation of Eosin Yellow adsorption onto Bottom Ash.

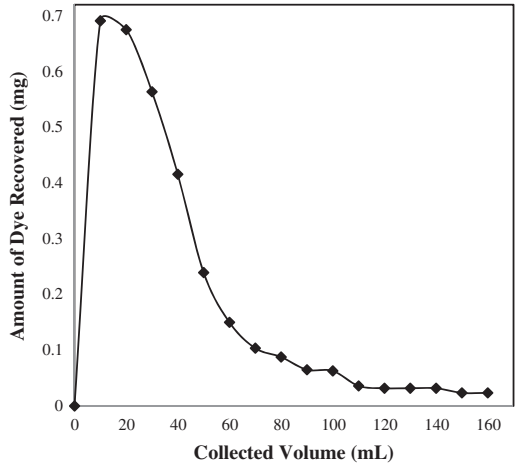

Fig. 12. Recovery of the Eosin Yellow from the exhausted column of Bottom Ash.

(Fig. 11). On the basis of Fig. 11, it was found that out of 8.99 mg of the dye taken in the original solution 3.58 mg dye was adsorbed over 1 g Bottom Ash and remaining 5.41 mg dyes came out through the column. Different column parameters calculated from above mentioned mathematical expressions are presented in Tables 5 and 6. It is interesting to note from Table 6 that the percentage saturation of Eosin Yellow over Bottom Ash column was found about 97%.

3.5.2. Column regeneration and dye recovery

To regenerate the exhausted adsorbent column and recover the adsorbed dye, desorption operations were carried out by eluting dilute NaOH solution through the exhausted column by maintaining a flow rate of 0.5 mL/min. The obtained desorption curve is presented in Fig. 12. It was observed that a large amount (about 77%) of the dye was removed by eluting first 40 ml NaOH solution and remaining amount of the dye was recovered in next 120 mL of the NaOH solution. Thus, total 160 mL of NaOH solution was sufficient to recover almost complete dye from the column and 90.32% recovery of the dye was achieved.

The adsorption efficiency was calculated by reloading the column with known concentration of Eosin Yellow. The breakthrough capacities during the first, second, third, and fourth cycles were found as 81, 73, 66, and 54%, respectively.

4. Conclusion

The present studies prove that Bottom Ash acts as a powerful scavenger for the eradication of Eosin Yellow dye from wastewater. The adsorption of Eosin Yellow over Bottom Ash is depending upon the pH of the solution, sieve size of adsorbent, amount of

adsorbent, adsorbate concentration, contact time, and temperature. The process is found to proceed via pseudo-second-order rate kinetics. Kinetic investigations also confirm the involvement of film diffusion process in the present case and activation energy and entropy of the process have been found as $3.748\,kJ\,Mol^{-1}$ and $477.764\,J\,K^{-1}\,Mol^{-1}$, respectively. It is also evaluated that the adsorption of Eosin Yellow over Bottom Ash obeys Langmuir, Freundlich, Tempkin, and D–R adsorption isotherms. Thermodynamic parameters obtained from the Langmuir isotherm data confirm the feasibility and spontaneity of the process, while values of separation factor "*r*" indicate the favorability of the ongoing adsorption process. Under the bulk removal Eosin Yellow is adsorbed through the fixed bed column of Bottom Ash. Attempts are also been made to recover the adsorbed dye by eluting dilute NaOH solution through exhausted columns.

Acknowledgment

One of the authors, DJ, thanks MANIT, Bhopal for providing financial assistance to carry out this work.

References

[1] B.M. Linde, Water on Earth, Bench Education, New York, NY, 2005.
[2] M.S. Reisch, Asian textile dye makers are a growing power in changing market, Chem. Eng. News 74(3) (1996) 10–12.
[3] Z. Aksu, Biosorption of reactive dyes by dried activated sludge: equilibrium and kinetic modelling, Biochem. Eng. J. 7 (2001) 79–84.
[4] P. MacCarthy, R.W. Klusman, S.W. Cowling, J.A. Rice, Water analysis, Anal. Chem. 67 (1995) 525R–582R.
[5] S.H. Lin, C.F. Peng, Treatment of textile wastewater by electrochemical method, Wat. Res. 28 (1994) 277–282.
[6] T. Kim, C. Park, S. Kim, Water recycling from desalination and purification process of reactive dye manufacturing industry by combined membrane filtration, J. Cleaner Prod. 13 (2005) 779–786.
[7] T. Robinson, B. Chandran, P. Nigam, Removal of dyes from a synthetic textile dye effluent by biosorption on apple pomace and wheat straw, Wat. Res. 36 (2002) 2824–2830.
[8] S. Raghu, C.A. Basha, Chemical or electrochemical techniques, followed by ion exchange, for recycle of textile dye wastewater, J. Hazard. Mater. 149(2) (2007) 324–330.
[9] E. Bizani, K. Fytionos, I. Poulios, V. Tsiridis, Photocatalytic decolorization and degradation of dye solution and wastewater in the presence of titanium dioxide, J. Hazard. Mater. 136 (2006) 85–94.
[10] V. Golob, A. Vinder, M. Simonic, Efficiency of the coagulation/Flocculation method for the treatment of dye bath effluents, Dyes Pigm. 67 (2005) 93–97.
[11] M. Kobya, O.T. Can, M. Bayramoglu, Treatment of textile wastewaters by electrocoagulation using iron and aluminum electrodes, J. Hazard. Mater. 100 (2003) 163–178.
[12] S.H. Lin, M.L. Chen, Combined ozonation and ion exchange treatment of textile wastewater effluents, J. Environ. Sci. Health 32 (1997) 1999–2010.
[13] H.N. Bhatti, N. Akram, And M Asgher, Optimization of culture conditions for enhanced decolorization of cibacron red FN-2BL by Schizophyllum commune IBL-6, Appl. Biochem. Biotechnol. 149(3) (2008) 255–264.
[14] H.N. Bhatti, R. Khalid, M.A. Hanif, Dynamic biosorption of Zn(II) and Cu(II) using pretreated *Rosa gruss an teplitz* (red rose) distillation sludge, Chem. Eng. J. 148(2–3) (2009) 434–443.
[15] H.N. Bhatti, A.W. Nasir, M.A. Hanif, Efficacy of *Daucus carota* L. waste biomass for the removal of chromium from aqueous solutions, Desalination 253(1–3) (2010) 78–87.
[16] I. Haq, H.N. Bhatti, M. Asgher, Removal of Solar red BA textile dye from aqueous solution by low cost barley husk: Equilibrium, kinetic and thermodynamic study, Can. J. Chem. Eng. 89 (2011) 593–600.
[17] Y. Safa, H.N. Bhatti, Kinetic and thermodynamic modeling for the removal of Direct Red-31 and Direct Orange-26 dyes from aqueous solutions by rice husk, Desalination 272 (2011) 313–322.
[18] M. Asgher, H.N. Bhatti, Removal of Reactive blue 19 and Reactive blue 49 textile dyes by citrus waste biomass from aqueous solution: equilibrium and kinetic study, Can. J. Chem. Eng. 90 (2012) 413–419.
[19] H.N. Bhatti, N. Akhtar, N. Saleem, Adsorptive removal of methylene blue by low cost Citrus sinensis bagasse: equilibrium, kinetic and thermodynamic characterization, The Arab. J. Sci. Eng. 37 (2012) 9–18.
[20] M. Asgher, H.N. Bhatti, Evaluation of thermodynamics and effect of chemical treatments on sorption potential of Citrus waste biomass for removal of anionic dyes from aqueous solutions, Ecol. Eng. 38 (2012) 79–85.
[21] H.N. Bhatti, Y. Safa, Removal of anionic dyes by rice milling waste from synthetic effluents: equilibrium and thermodynamic studies, Desalin. Water Treat. 48 (2012) 267–277.
[22] B.S. Girgis, L.B. Khalil, T.A.M. Tawfik, Activated carbon from sugarcane bagasse by carbonization in the presence of inorganic acids, J. Chem. Technol. Biotech. 61 (1994) 87–92.
[23] G. McKay, Application of surface diffusion model to the adsorption of dyes on bagasse pith, Adsorption 4 (1998) 361–372.
[24] N. Sakkayawong, P. Thiravetyan, W. Nakbanpote, Adsorption mechanism of synthetic reactive dye wastewater by chitosan, J. Colliod Interface Sci. 286 (2005) 36–42.
[25] B.H. Hameed, Spent tea leaves: A new non-conventional and low-cost adsorbent for removal of basic dye from aqueous solutions, J. Hazard. Mater. 161 (2009) 753–759.
[26] W. Shi, X. Xu, G. Sun, Chemically modified sunflower stalks as adsorbents for color removal from textile wastewater, J. Appl. Polym. Sci. 71 (1999) 1841–1850.
[27] http://en.wikipedia.org/wiki/Fluorescein (accessed 19 March 2013).
[28] http://www.pubmedcentral.nih.gov/articlerender.fcgi?tool=pmcentrez&artid=1831125 (accessed 19 March 2013).
[29] P. Argueso, A. Tisdale, S. Spurr-Michaud, I.K. Gipson, Mucin characteristics of human corneal- Limbal epithelial cells that exclude the rose Bengal anionic dye, Invest. Ophthalmol. Vis. Sci. 47(1) (2006) 113–119.
[30] L. Ganesan, E. Margolles-Clark, Y. Song, P. Buchwald, The food colorant erythrosine is a promiscuous protein-protein interaction inhibitor, Biochem. Pharmacol. 81 (2011) 810–818.
[31] R.D. Combes, R.B. Haveland-Smith, A Review of the Genotoxicity of Food, Drug and Cosmetic Colors and other Azo Tiphenylmethane and Xanthenes Dyes, Mut. Res./Rev. Gen. Toxicol. 98 (1982) 101–243.
[32] M. Kersten, B. Schulz-Dobrick, T. Lichtensteiger, C.A. Johnson, Speciation of Cr in leachates of a MSWI bottom ash landfill, Environ. Sci. Technol. 32 (1998) 1398–1403.
[33] C.C. Carlson, D.C. Adriano, Environmental impacts of coal combustion residues, J. Environ. Qual. 22 (1993) 227–247.
[34] A.I. Vogel, (Ed.), Vogel's Textbook of Quantitative Chemical Analysis, fifth ed., Longman, London, 1989.

[35] Y.S. Ho, G. McKay, Kinetic model of lead (II) sorption onto peat, Adsorp. Sci. Technol. 16 (1998) 243–255.
[36] A. Mittal, J. Mittal, L. Kurup, A.K. Singh, Process development for the removal and recovery of hazardous dye erythrosine from wastewater by waste materials—bottom ash and de-oiled soya as adsorbents, J. Hazard. Mater. 138(1) (2006) 95–105.
[37] A. Mittal, D. Kaur, J. Mittal, Batch and bulk removal of a triarymethane dye, fast green fcf, from wastewater by adsorption over waste materials, J. Hazard. Mater. 163 (2009) 568–577.
[38] A. Mittal, D. Kaur, J. Mittal, Applicability of waste materials—bottom ash and de-oiled soya, as adsorbents for the removal and recovery of a hazardous dye—brilliant green, J. Colliod Interface Sci. 326 (2008) 8–17.
[39] G.E. Boyd, A.W. Adamson, L.S. Meyers, The exchange adsorption of ions from aqueous solution by organic zeolites. III. Performance of deep adsorbent beds under non-equilibrium conditions, J. Am. Chem. Soc. 69 (1947) 2849–2859.
[40] D. Reichenberg, Properties of ion exchange resins in relation to their structure III kinetics of exchange, J. Am. Chem. Soc. 75 (1953) 589–597.
[41] A. Mittal, D. Kaur, A. Malviya, J. Mittal, V.K. Gupta, Adsorption studies on the removal of coloring agent Phenol Red from wastewater using waste materials as adsorbents, J. Colliod Interface Sci. 337(2) (2009) 345–354.
[42] A. Mittal, J. Mittal, A. Malviya, D. Kaur, V.K. Gupta, Adsorption of hazardous dye Crystal Violet from wastewater by waste materials, J. Colliod Interface Sci. 343 (2010) 463–473.
[43] S.Q. Memon, N. Memon, A.R. Solangi, J. Memon, Sawdust: A green and economical sorbent for thallium removal, Chem. Eng. J. 140 (2008) 235–240.
[44] T.W. Weber, R.K. Chakravorti, Pore and solid diffusion models for fixed bed adsorbers, J. Am. Inst. Chem. Eng. 20 (1974) 228–238.
[45] A.S. Michaels, Breakthrough curves in ion–exchange, Ind. Eng. Chem. 44 (1952) 1922–1930.